

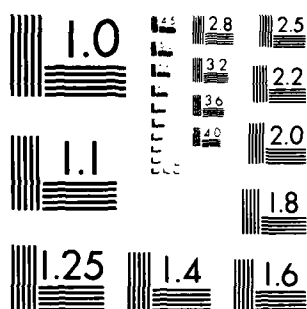
AD-A130 101

FINAL REPORT ON AFOSR-81-0042(U) BOSTON UNIV MA CENTER 1/1
FOR POLYMER STUDIES H E STANLEY SEP 82
AFOSR-TR-83-0570 AFOSR-81-0042

UNCLASSIFIED

F/G 12/1 NL

												END DATE FILMED 7-83 DTIC	



MICROCOPY RESOLUTION TEST CHART
NATIONAL BUREAU OF STANDARDS-1963-A

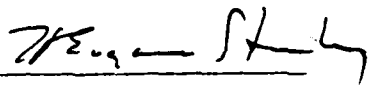
AFOSR-TR- 83-0570

ADA130101

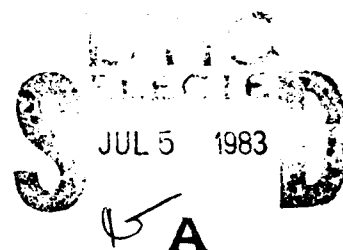
GRANT AFOSR # 81-0042

Air Force Office of Scientific Research
FINAL REPORT

Period Covered: 10/1/81 - 9/30/82


H. Eugene Stanley
University Professor
Director, Center for Polymer Studies

PRINCIPAL INVESTIGATOR



DTIC FILE COPY

Approved for public release:
distribution unlimited.

83 07 01 018

UNCLASSIFIED

SECURITY CLASSIFICATION OF THIS PAGE (When Data Entered)

REPORT DOCUMENTATION PAGE		READ INSTRUCTIONS BEFORE COMPLETING FORM
1. REPORT NUMBER AFOSR-TR- 83-0570	2. GOVT ACCESSION NO.	3. RECIPIENT'S CATALOG NUMBER
4. TITLE (and Subtitle) FINAL REPORT ON AFOSR-81-0042		5. TYPE OF REPORT & PERIOD COVERED Final Report 10/1/81-9/30/82
		6. PERFORMING ORG. REPORT NUMBER
7. AUTHOR(s) H. Eugene Stanley		8. CONTRACT OR GRANT NUMBER(s) AFOSR - 81-0042
9. PERFORMING ORGANIZATION NAME AND ADDRESS Center for Polymer Studies Boston University 111 Cummington Street, Boston, MA 02215		10. PROGRAM ELEMENT, PROJECT, TASK AREA & WORK UNIT NUMBERS 61102F / 2301-A5 2403-18
11. CONTROLLING OFFICE NAME AND ADDRESS AFOSR/INP Bolling Air Force Base, Washington, D.C. 20332		12. REPORT DATE <i>Sep 1982</i>
		13. NUMBER OF PAGES 22
14. MONITORING AGENCY NAME & ADDRESS (if different from Controlling Office)		15. SECURITY CLASS. (of this report) Unclassified
		15a. DECLASSIFICATION DOWNGRADING SCHEDULE
16. DISTRIBUTION STATEMENT (of this Report) Approved for publication release; distribution unlimited		
17. DISTRIBUTION STATEMENT (of the abstract entered in Block 20, if different from Report)		
18. SUPPLEMENTARY NOTES		
19. KEY WORDS (Continue on reverse side if necessary and identify by block number)		
20. ABSTRACT (Continue on reverse side if necessary and identify by block number) A statistical-mechanical model for reversible gelation is developed. This model takes into account solvent effects, which usually are neglected in the classical theory of gelation. The exact solution of this model is given for the limiting case in which "loops" or intermolecular interactions may be neglected (Cayley tree). The general phase diagram is obtained and it is shown that, with a particular choice of a solvent, one can realize the interesting situation in which gelation point and consolute		

DD FORM 1 JAN 73 1473

EDITION OF 1 NOV 65 IS OBSOLETE

UNCLASSIFIED

SECURITY CLASSIFICATION OF THIS PAGE (When Data Entered)

UNCLASSIFIED

SECURITY CLASSIFICATION OF THIS PAGE(When Data Entered)

↓
point coincide. This point has peculiar properties associated with the simultaneous divergence of "connectivity" and thermal fluctuations. The recent experimental data of Tanaka and collaborators are in good qualitative agreement with the predictions of the model.
↑

UNCLASSIFIED

SECURITY CLASSIFICATION OF THIS PAGE(When Data Entered)

A. INVESTIGATIONS OF THE SOL-GEL TRANSITION

A new critical line in a model for the sol-gel transition

Site-bond correlated percolation has been recently introduced by our group, as a model to study solvent effects in the sol-gel transition. This model has stimulated further research because of its interesting behavior. In particular, Delyon, Souillard and Stauffer have found a line of percolation transitions without the appearance of an infinite cluster, similar to the Griffiths singularity in a dilute ferromagnet. We have complemented this study and shown that there is another line of critical points where the pair-connectedness function becomes critical without the disappearance of the infinite cluster. The physical consequence of such a critical line is the formation of a gel with a network structure completely different from most physical gels.

Migdal-Kadanoff renormalization group analysis for a sol-gel transition model

The site-bond Ising correlated percolation model is not easily analyzed, particularly in 3 dimensions. This is due to the difficulty in satisfying the Ising symmetry and the connectivity properties. In order to circumvent this problem, we have carried out an analysis using the Migdal-Kadanoff R.G. We have proposed an alternative scheme which gives good results for the random-site-bond percolation problem. We intend to generalize this procedure to the correlated case.

Study of droplets for a statistical mechanical model of gelation in three dimensions

Using a Monte Carlo simulation, we have studied the droplet size distribution for the Ising correlated site-bond percolation problem in three dimensions. The exponent for that distribution is found to agree well with the corresponding

ADDITIONAL INFORMATION
1.
2.
3.
4.
5.
6.
7.
8.
9.
10.
11.
12.
13.
14.
15.
16.
17.
18.
19.
20.
21.
22.
23.
24.
25.
26.
27.
28.
29.
30.
31.
32.
33.
34.
35.
36.
37.
38.
39.
40.
41.
42.
43.
44.
45.
46.
47.
48.
49.
50.
51.
52.
53.
54.
55.
56.
57.
58.
59.
60.
61.
62.
63.
64.
65.
66.
67.
68.
69.
70.
71.
72.
73.
74.
75.
76.
77.
78.
79.
80.
81.
82.
83.
84.
85.
86.
87.
88.
89.
90.
91.
92.
93.
94.
95.
96.
97.
98.
99.
100.
101.
102.
103.
104.
105.
106.
107.
108.
109.
110.
111.
112.
113.
114.
115.
116.
117.
118.
119.
120.
121.
122.
123.
124.
125.
126.
127.
128.
129.
130.
131.
132.
133.
134.
135.
136.
137.
138.
139.
140.
141.
142.
143.
144.
145.
146.
147.
148.
149.
150.
151.
152.
153.
154.
155.
156.
157.
158.
159.
160.
161.
162.
163.
164.
165.
166.
167.
168.
169.
170.
171.
172.
173.
174.
175.
176.
177.
178.
179.
180.
181.
182.
183.
184.
185.
186.
187.
188.
189.
190.
191.
192.
193.
194.
195.
196.
197.
198.
199.
200.
201.
202.
203.
204.
205.
206.
207.
208.
209.
210.
211.
212.
213.
214.
215.
216.
217.
218.
219.
220.
221.
222.
223.
224.
225.
226.
227.
228.
229.
230.
231.
232.
233.
234.
235.
236.
237.
238.
239.
240.
241.
242.
243.
244.
245.
246.
247.
248.
249.
250.
251.
252.
253.
254.
255.
256.
257.
258.
259.
260.
261.
262.
263.
264.
265.
266.
267.
268.
269.
270.
271.
272.
273.
274.
275.
276.
277.
278.
279.
280.
281.
282.
283.
284.
285.
286.
287.
288.
289.
290.
291.
292.
293.
294.
295.
296.
297.
298.
299.
300.
301.
302.
303.
304.
305.
306.
307.
308.
309.
310.
311.
312.
313.
314.
315.
316.
317.
318.
319.
320.
321.
322.
323.
324.
325.
326.
327.
328.
329.
330.
331.
332.
333.
334.
335.
336.
337.
338.
339.
340.
341.
342.
343.
344.
345.
346.
347.
348.
349.
350.
351.
352.
353.
354.
355.
356.
357.
358.
359.
360.
361.
362.
363.
364.
365.
366.
367.
368.
369.
370.
371.
372.
373.
374.
375.
376.
377.
378.
379.
380.
381.
382.
383.
384.
385.
386.
387.
388.
389.
390.
391.
392.
393.
394.
395.
396.
397.
398.
399.
400.
401.
402.
403.
404.
405.
406.
407.
408.
409.
410.
411.
412.
413.
414.
415.
416.
417.
418.
419.
420.
421.
422.
423.
424.
425.
426.
427.
428.
429.
430.
431.
432.
433.
434.
435.
436.
437.
438.
439.
440.
441.
442.
443.
444.
445.
446.
447.
448.
449.
450.
451.
452.
453.
454.
455.
456.
457.
458.
459.
460.
461.
462.
463.
464.
465.
466.
467.
468.
469.
470.
471.
472.
473.
474.
475.
476.
477.
478.
479.
480.
481.
482.
483.
484.
485.
486.
487.
488.
489.
490.
491.
492.
493.
494.
495.
496.
497.
498.
499.
500.
501.
502.
503.
504.
505.
506.
507.
508.
509.
510.
511.
512.
513.
514.
515.
516.
517.
518.
519.
520.
521.
522.
523.
524.
525.
526.
527.
528.
529.
530.
531.
532.
533.
534.
535.
536.
537.
538.
539.
540.
541.
542.
543.
544.
545.
546.
547.
548.
549.
550.
551.
552.
553.
554.
555.
556.
557.
558.
559.
560.
561.
562.
563.
564.
565.
566.
567.
568.
569.
570.
571.
572.
573.
574.
575.
576.
577.
578.
579.
580.
581.
582.
583.
584.
585.
586.
587.
588.
589.
590.
591.
592.
593.
594.
595.
596.
597.
598.
599.
600.
601.
602.
603.
604.
605.
606.
607.
608.
609.
610.
611.
612.
613.
614.
615.
616.
617.
618.
619.
620.
621.
622.
623.
624.
625.
626.
627.
628.
629.
630.
631.
632.
633.
634.
635.
636.
637.
638.
639.
640.
641.
642.
643.
644.
645.
646.
647.
648.
649.
650.
651.
652.
653.
654.
655.
656.
657.
658.
659.
660.
661.
662.
663.
664.
665.
666.
667.
668.
669.
670.
671.
672.
673.
674.
675.
676.
677.
678.
679.
680.
681.
682.
683.
684.
685.
686.
687.
688.
689.
690.
691.
692.
693.
694.
695.
696.
697.
698.
699.
700.
701.
702.
703.
704.
705.
706.
707.
708.
709.
710.
711.
712.
713.
714.
715.
716.
717.
718.
719.
720.
721.
722.
723.
724.
725.
726.
727.
728.
729.
730.
731.
732.
733.
734.
735.
736.
737.
738.
739.
740.
741.
742.
743.
744.
745.
746.
747.
748.
749.
750.
751.
752.
753.
754.
755.
756.
757.
758.
759.
760.
761.
762.
763.
764.
765.
766.
767.
768.
769.
770.
771.
772.
773.
774.
775.
776.
777.
778.
779.
780.
781.
782.
783.
784.
785.
786.
787.
788.
789.
790.
791.
792.
793.
794.
795.
796.
797.
798.
799.
800.
801.
802.
803.
804.
805.
806.
807.
808.
809.
810.
811.
812.
813.
814.
815.
816.
817.
818.
819.
820.
821.
822.
823.
824.
825.
826.
827.
828.
829.
830.
831.
832.
833.
834.
835.
836.
837.
838.
839.
840.
841.
842.
843.
844.
845.
846.
847.
848.
849.
850.
851.
852.
853.
854.
855.
856.
857.
858.
859.
860.
861.
862.
863.
864.
865.
866.
867.
868.
869.
870.
871.
872.
873.
874.
875.
876.
877.
878.
879.
880.
881.
882.
883.
884.
885.
886.
887.
888.
889.
890.
891.
892.
893.
894.
895.
896.
897.
898.
899.
900.
901.
902.
903.
904.
905.
906.
907.
908.
909.
910.
911.
912.
913.
914.
915.
916.
917.
918.
919.
920.
921.
922.
923.
924.
925.
926.
927.
928.
929.
930.
931.
932.
933.
934.
935.
936.
937.
938.
939.
940.
941.
942.
943.
944.
945.
946.
947.
948.
949.
950.
951.
952.
953.
954.
955.
956.
957.
958.
959.
960.
961.
962.
963.
964.
965.
966.
967.
968.
969.
970.
971.
972.
973.
974.
975.
976.
977.
978.
979.
980.
981.
982.
983.
984.
985.
986.
987.
988.
989.
990.
991.
992.
993.
994.
995.
996.
997.
998.
999.
1000.
1001.
1002.
1003.
1004.
1005.
1006.
1007.
1008.
1009.
1010.
1011.
1012.
1013.
1014.
1015.
1016.
1017.
1018.
1019.
1020.
1021.
1022.
1023.
1024.
1025.
1026.
1027.
1028.
1029.
1030.
1031.
1032.
1033.
1034.
1035.
1036.
1037.
1038.
1039.
1040.
1041.
1042.
1043.
1044.
1045.
1046.
1047.
1048.
1049.
1050.
1051.
1052.
1053.
1054.
1055.
1056.
1057.
1058.
1059.
1060.
1061.
1062.
1063.
1064.
1065.
1066.
1067.
1068.
1069.
1070.
1071.
1072.
1073.
1074.
1075.
1076.
1077.
1078.
1079.
1080.
1081.
1082.
1083.
1084.
1085.
1086.
1087.
1088.
1089.
1090.
1091.
1092.
1093.
1094.
1095.
1096.
1097.
1098.
1099.
1100.
1101.
1102.
1103.
1104.
1105.
1106.
1107.
1108.
1109.
1110.
1111.
1112.
1113.
1114.
1115.
1116.
1117.
1118.
1119.
1120.
1121.
1122.
1123.
1124.
1125.
1126.
1127.
1128.
1129.
1130.
1131.
1132.
1133.
1134.
1135.
1136.
1137.
1138.
1139.
1140.
1141.
1142.
1143.
1144.
1145.
1146.
1147.
1148.
1149.
1150.
1151.
1152.
1153.
1154.
1155.
1156.
1157.
1158.
1159.
1160.
1161.
1162.
1163.
1164.
1165.
1166.
1167.
1168.
1169.
1170.
1171.
1172.
1173.
1174.
1175.
1176.
1177.
1178.
1179.
1180.
1181.
1182.
1183.
1184.
1185.
1186.
1187.
1188.
1189.
1190.
1191.
1192.
1193.
1194.
1195.
1196.
1197.
1198.
1199.
1200.
1201.
1202.
1203.
1204.
1205.
1206.
1207.
1208.
1209.
1210.
1211.
1212.
1213.
1214.
1215.
1216.
1217.
1218.
1219.
1220.
1221.
1222.
1223.
1224.
1225.
1226.
1227.
1228.
1229.
1230.
1231.
1232.
1233.
1234.
1235.
1236.
1237.
1238.
1239.
1240.
1241.
1242.
1243.
1244.
1245.
1246.
1247.
1248.
1249.
1250.
1251.
1252.
1253.
1254.
1255.
1256.
1257.
1258.
1259.
1260.
1261.
1262.
1263.
1264.
1265.
1266.
1267.
1268.
1269.
1270.
1271.
1272.
1273.
1274.
1275.
1276.
1277.
1278.
1279.
1280.
1281.
1282.
1283.
1284.
1285.
1286.
1287.
1288.
1289.
1290.
1291.
1292.
1293.
1294.
1295.
1296.
1297.
1298.
1299.
1300.
1301.
1302.
1303.
1304.
1305.
1306.
1307.
1308.
1309.
1310.
1311.
1312.
1313.
1314.
1315.
1316.
1317.
1318.
1319.
1320.
1321.
1322.
1323.
1324.
1325.
1326.
1327.
1328.
1329.
1330.
1331.
1332.
1333.
1334.
1335.
1336.
1337.
1338.
1339.
1340.
1341.
1342.
1343.
1344.
1345.
1346.
1347.
1348.
1349.
1350.
1351.
1352.
1353.
1354.
1355.
1356.
1357.
1358.
1359.
1360.
1361.
1362.
1363.
1364.
1365.
1366.
1367.
1368.
1369.
1370.
1371.
1372.
1373.
1374.
1375.
1376.
1377.
1378.
1379.
1380.
1381.
1382.
1383.
1384.
1385.
1386.
1387.
1388.
1389.
1390.
1391.
1392.
1393.
1394.
1395.
1396.
1397.
1398.
1399.
1400.
1401.
1402.
1403.
1404.
1405.
1406.
1407.
1408.
1409.
1410.
1411.
1412.
1413.
1414.
1415.
1416.
1417.
1418.
1419.
1420.
1421.
1422.
1423.
1424.
1425.
1426.
1427.
1428.
1429.
1430.
1431.
1432.
1433.
1434.
1435.
1436.
1437.
1438.
1439.
1440.
1441.
1442.
1443.
1444.
1445.
1446.
1447.
1448.
1449.
1450.
1451.
1452.
1453.
1454.
1455.
1456.
1457.
1458.
1459.
1460.
1461.
1462.
1463.
1464.
1465.
1466.
1467.
1468.
1469.
1470.
1471.
1472.
1473.
1474.
1475.
1476.
1477.
1478.
1479.
1480.
1481.
1482.
1483.
1484.
1485.
1486.
1487.
1488.
1489.
1490.
1491.
1492.
1493.
1494.
1495.
1496.
1497.
1498.
1499.
1500.
1501.
1502.
1503.
1504.
1505.
1506.
1507.
1508.
1509.
1510.
1511.
1512.
1513.
1514.
1515.
1516.
1517.
1518.
1519.
1520.
1521.
1522.
1523.
1524.
1525.
1526.
1527.
1528.
1529.
1530.
1531.
1532.
1533.
1534.
1535.
1536.
1537.
1538.
1539.
1540.
1541.
1542.
1543.
1544.
1545.
1546.
1547.
1548.
1549.
1550.
1551.
1552.
1553.
1554.
1555.
1556.
1557.
1558.
1559.
1560.
1561.
1562.
1563.
1564.
1565.
1566.
1567.
1568.
1569.
1570.
1571.
1572.
1573.
1574.
1575.
1576.
1577.
1578.
1579.
1580.
1581.
1582.
1583.
1584.
1585.
1586.
1587.
1588.
1589.
1590.
1591.
1592.
1593.
1594.
1595.
1596.
1597.
1598. <

exponent of the Ising model. We also have discussed the relation between the susceptibility and the second moment by using the dilute Potts formulation of this percolation problem.

B. STRUCTURE OF BRANCHED POLYMERS

Branched polymer in a solvent

A model for branched polymers in a solvent is studied as a function of three parameters: the chemical potential of the sites, the chemical potential of the bonds, and the nearest-neighbor interaction amongst the sites. We have shown that this problem can be mapped into a generalized percolation problem. A Potts formalism for this problem can be formulated to which the Migdal-Kadanoff RG has been applied. We have found a surface of critical points corresponding to a randomly-branched polymer (or random animal), a line of tricritical points corresponding to a polymer collapse (θ -point), a higher order critical point which corresponds to percolation, and a first-order phase transition which corresponds to a compact polymer. The critical surface terminates at the θ -line, and the θ -line ends at the percolation point. This new prediction of a higher-order percolation point where the branched polymer changes its structure is amenable to experimental and computer verification.

Flory theory for directed branched polymers

We have applied the Flory theory to branched polymeric systems in which there is a preferential direction for polymerization to occur. This anisotropy gives rise to new types of critical behavior that can be accounted for accurately and quite simply by a Flory approach. Specifically, we find an upper critical spatial dimension of $d = d_c = 7$ and correlation length exponents of

$$\nu_{\parallel} = (d + 11)/4(d + 2) \quad \nu_{\perp} = 9/16/(d + 2)$$

parallel and perpendicular to the anisotropy respectively.

C. NUCLEATION AND SPINODAL DECOMPOSITION

One of the more interesting and important (from a materials viewpoint) areas of polymer physics is the study of metastable polymers. Both nucleation and growth and spinodal decomposition are important mechanisms by which polymeric materials are formed. We have begun an integrated experimental and theoretical program to understand nucleation and growth and spinodal decomposition in polymer systems.

Spinodals in medium-range systems

Although the spinodal concept has been questioned, it has been useful in understanding experimental data in polymer systems, and we have begun to study such medium-range interactions in continuum systems. No evidence of a spinodal was found, but we were able to show that pseudospinodals (i.e., extrapolations into the metastable region) converge rapidly with the interaction range to the true spinodal (if it exists). We also observed, for the first time, a breakdown of the classical droplet model.

The research done so far is in lattice systems. To make our studies more realistic we have begun to examine continuum systems. The interaction between the particles is chosen to be a hard-core potential with an additional attractive square well. If the spinodal line exists, the compressibility should diverge as this line is approached.

For short-range interactions, as the metastable region is probed, the system

becomes becomes unstable before the predicted spinodal line is reached. To facilitate a deeper probe into the metastable region, the interaction range is extended by increasing the width of the attractive well. The compressibility is then measured as a function of both density and interaction range.

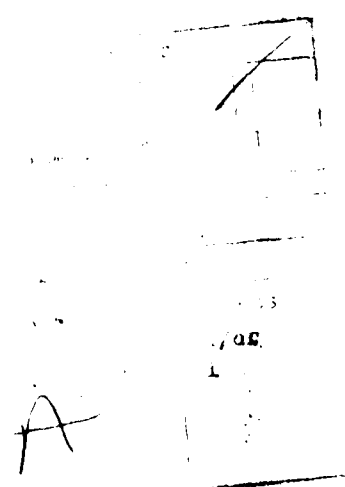
Dynamics of supercooled fluids and polymer melts

We have investigated the dynamics of supercooled fluids and polymer melts based on a static mean-field theory of freezing developed by Grewe and Klein, and the dynamical theory of Cahn and Hilliard. A nonlocal term is introduced into the standard Landau-Ginsberg-Wilson Hamiltonian and the resulting dynamics are explored. It is shown that for short times the supercooled liquid is unstable to density fluctuations of nonzero wavevector k . The value of k at which this instability first appears is on the order of the inverse range of the interaction potential.

MANUSCRIPTS SUBMITTED OR PUBLISHED UNDER AFOSR SPONSORSHIP

DURING THE PERIOD 1 OCTOBER 1981 - 30 SEPTEMBER 1982

A. Coniglio, H. E. Stanley and W. Klein, "Solvent effects on polymer gels: A statistical-mechanical model," Phys. Rev. B 25, 6805-6821 (1982).



Solvent effects on polymer gels: A statistical-mechanical model

A. Coniglio,* H. E. Stanley, and W. Klein

Center for Polymer Studies and Department of Physics, Boston University, Boston, Massachusetts 02215

(Received 1 February 1982)

A statistical-mechanical model for reversible gelation is developed. This model takes into account solvent effects, which usually are neglected in the classical theory of gelation. The exact solution of this model is given for the limiting case in which "loops" or intermolecular interactions may be neglected (Cayley tree). The general phase diagram is obtained and it is shown that, with a particular choice of a solvent, one can realize the interesting situation in which gelation point and consolute point coincide. This point has peculiar properties associated with the simultaneous divergence of "connectivity" and thermal fluctuations. The recent experimental data of Tanaka and collaborators are in good qualitative agreement with the predictions of the model.

I. INTRODUCTION

Much of the progress of the last decade in statistical mechanics stems from the fact that relatively simple and therefore tractable models have proved sufficient to describe extremely subtle cooperative phenomena. Three examples are shown schematically in Fig. 1:

(i) *A fluid near its critical point.* The Ising or lattice-gas model¹ has proved remarkably successful in interpreting a wide range of data near the critical points of fluids.² This stems from the fact that the "essential physics" of the problem is an interparticle interaction potential characterized by a hard-core repulsion and a short-range attraction.

(ii) *Dilute and semidilute polymer solutions.* The $n=0$ limit of the n -vector model has proved capable of describing polymer solutions in the dilute³ and semidilute⁴ regimes, where the magnetic field plays the role of concentration.⁵

(iii) *Polymer gelation.* The essential physical feature of a gel is connectivity, and hence one expects percolation phenomena to be relevant.⁶ As we shall see, temperature-dependent effects such as those due to the presence of solvent are excluded from simple "pure percolation."⁷ It is the purpose of this paper to suitably generalize pure percolation in order to incorporate such effects.⁸

In Sec. II we shall describe our approach using polyfunctional condensation, the simplest example that illustrates the basic phenomenon of gelation. In Sec. III we derive the equation of state, while in Sec. IV we describe the connectivity properties. Then in Sec. V we describe the more general gelation of "vulcanization" phenomena in which poly-

mers made up of M monomers are permitted to crosslink. The detailed derivation of the appropriate formula are given in Appendixes A and B.

II. THE MODEL ($M=1$)

We shall first describe our model for the simplest case of gelation, the polyfunctional condensation of f -functional monomers. Suppose all the monomers are identical, and that each has f -functional groups that can react with one of the f groups of another monomer. The simplest case, $f=0$, produces no reactions at all. The next simplest case, $f=1$, results in dimers only. If $f=2$, we can have unbranched linear polymers. For $f>3$, we form branched polymers, as illustrated in

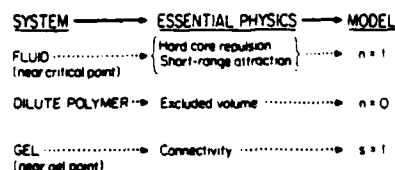


FIG. 1. Schematic illustration of the application of specific model Hamiltonians to capture the essential physics embodied by various physical systems near their respective critical points. The symbol n refers to the number of components of the order parameter in an n -vector model (isotropically interacting n -dimensional classical spins), while the symbol s refers to the number of discrete states in a s -state Potts model. The "critical point" of a dilute polymer solution corresponds to the limit $N \rightarrow \infty$, where N is the polymerization index.

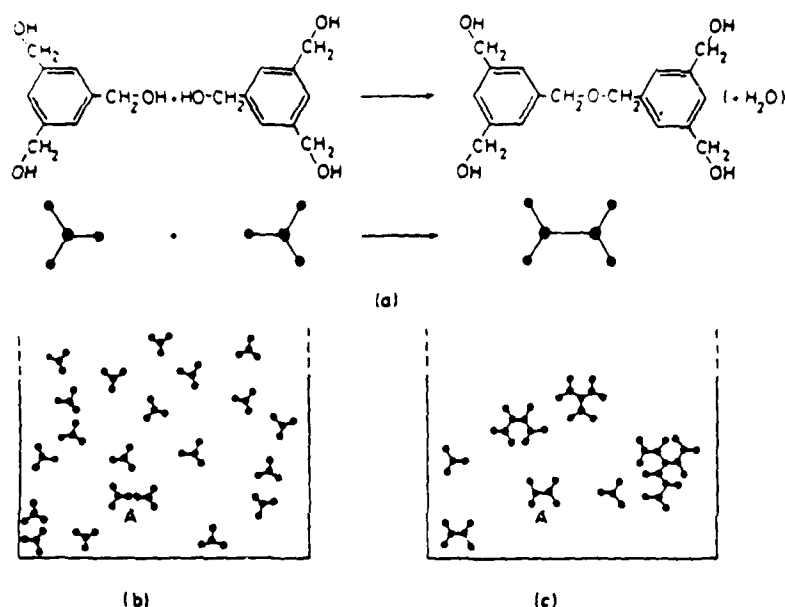


FIG. 2. Illustration of the simplest gelation phenomenon, polyfunctional condensation of f -functional monomers. The f -functional monomer shown in (a) is trimethylol benzene; it has three "functional" groups which can react to form ether linkages. If f were 2, then the most complex structures possible would be chains and rings. However, since $f > 2$ here, there exists the possibility of forming branched networks. In (b) and (c) are shown beakers at successive stages of reaction. This figure is from Gordon and Ross-Murphy (Ref. 9).

Fig. 2 for a particular example with $f = 3$, trimethylol benzene.⁹ Each benzene ring has three groups that can react to form an ester linkage. This process is characterized by a single parameter α , termed the conversion, which is the fraction of reacted groups. Clearly if $\alpha = 0$, only monomers are present. If $0 < \alpha < 1$, there exists a distribution of finite polymers of all possible sizes. However, the probability of an infinite polymer or "gel" is zero for all values of less than a critical value α_c . For $\alpha > \alpha_c$, there is a nonzero probability for the occurrence of a single branched polymer that is infinite in spatial extent. Thus the probability of the gel molecule to occur jumps discontinuously from zero for $\alpha < \alpha_c$ to unity for $\alpha > \alpha_c$, and hence the connectivity of the system changes drastically at $\alpha = \alpha_c$. This "phase transition" is termed the gelation threshold.

The first successful model to capture the essential physics of the gelation threshold was proposed 40 years ago by Flory and developed in a series of classic papers by both Flory¹⁰ and Stockmayer.¹¹ (Also see the classic book by Flory.¹²) This "Flory-Stockmayer" (FS) model not only predicts the occurrence of a gelation threshold $\alpha = \alpha_c$, but

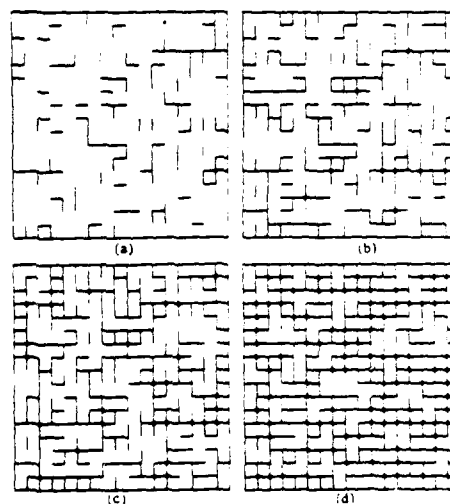


FIG. 3. Phenomenon of bond percolation: a finite section (16×16) of an infinite "fence," in which a fraction p_B of the links are conducting while the remaining fraction $q_B = 1 - p_B$ are insulating. Four choices of the parameter p_B are shown: (a) $p_B = 0.2$, (b) $p_B = 0.4$, (c) $p_B = 0.6$, and (d) $p_B = 0.8$.

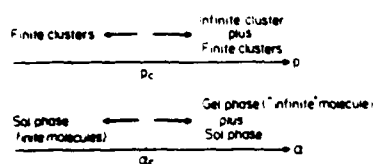


FIG. 4. Analogy between the phase diagrams of pure bond percolation and polyfunctional condensation (gelation of f -functional monomers). The role of p in gelation is played by α , which is termed the "conversion" or "extent of reaction"; it may be thought of as the fraction of intact bonds.

also provides precise predictions for the family of critical-point exponents characterizing the behavior of various quantities in the immediate vicinity of α_c .

For the purposes of this paper it is most appropriate to explain the FS model in the context of random-bond percolation, which in turn is illustrated in Fig. 3. Suppose we have an infinitely high and infinitely long wire fence. Imagine also that a randomly chosen fraction p_B of the links of this fence are conducting while the remaining fraction $(1-p_B)$ are insulating. Computer simulations of a finite (16×16) section of this fence are shown in Fig. 3 for $p_B = 0.2, 0.4, 0.6$, and 0.8 .

Clearly, for p_B small, as in Fig. 3(a), the system consists of small clusters of conducting bonds. In 3(b) the conducting fraction p_B has doubled, yet the system still consists of only finite clusters—the "scale" has increased, but not the essential macroscopic conductivity. In 3(c), $p_B = 0.6$, and the system is macroscopically different: In addition to the finite clusters, there is a single cluster that is infinite in spatial extent (of course, the fence must be infinite if the cluster is to be infinite). For some value of p_B in between Figs. 3(b) and 3(c), there is a threshold p_B^c ; below p_B^c the fence cannot conduct, while above p_B^c it can. Thus its macroscopic properties change suddenly as a microscopic parameter p_B increases infinitesimally from $p_B^c - \delta$ to $p_B^c + \delta$ [Fig. 4(a)].

Similarly, below the gelation threshold α_c , the system of Fig. 2 consists of only finite-size polymers; it cannot, e.g., sustain a shear stress. Above the threshold it can. Thus the macroscopic properties change suddenly as a microscopic parameter α , the extent of reaction (or equivalently, the fraction of formed crosslinks), increases infinitesimally from $\alpha_c - \delta$ to $\alpha_c + \delta$ [Fig. 4(b)].

The FS model was formulated in a fashion that

at first sight seems to be lattice independent: One only requires that a given polymer be forbidden to loop back upon itself. In short, "intramolecular interactions" are excluded. This assumption is fully equivalent (as far as critical behavior is concerned) to the statement that the polyfunctional monomers be required to occupy the sites of a Cayley-tree pseudolattice: To each configuration of the f -functional monomers there is a one-to-one correspondence with a configuration of bonds on the Cayley tree with coordination number $z = f$.

The effect of allowing for loops is clear, at least on a qualitative level. Clearly the threshold is expected to increase, since extra bonds will be formed that will merely create a loop rather than contributing to the formation of an infinite branched network. Moreover, we expect that the behavior of the system in the immediate vicinity of the gel point to be characterized by different critical exponents. In fact, if we are to believe the utility of lattice models, then it turns out that exponents are shifted from their Cayley-tree values quite considerably (Fig. 5). Of course, one could well question the appropriateness of a lattice model to represent a continuum system.^{13,14} Hence much needed are calculations for "continuum percolation" that are sufficiently accurate to make meaningful predictions concerning critical-point exponents.

Experimental evidence for departures for "classical" critical-point exponents is somewhat inconclusive at the present time. A literature search focused on this question was recently carried out by Brauner,¹⁵ who concluded that no clear-cut answer emerges despite rather extensive analysis of

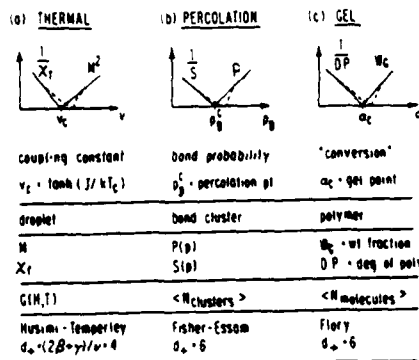


FIG. 5. Illustration of the analogies between (a) an ordinary thermal phase transition (e.g., an Ising or lattice-gas model), (b) bond percolation, and (c) polyfunctional condensation.

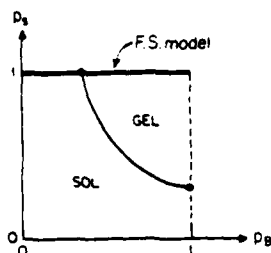


FIG. 6. Schematic phase diagram of random-site, random-bond percolation, where p_s is the site occupation probability and p_b is the probability that a randomly chosen bond is found to be intact.

existing data. A recent set of experiments by Schmidt and Burchard suggests that the Cayley-tree predictions may be quite adequate.¹⁶ However, problems arise due to the paucity of data extremely close to the gel point—since only there are exponents expected to depart from their classical values.¹⁷

In the FS model solvent effects are not included. Nor are temperature effects included in any statistical mechanical fashion: All states of a system consisting of b occupied bonds are equally probable. This simplifying feature has great merit in that the FS model is extremely tractable.

In FS theory all sites are occupied by monomers. However, we know that solvent effects are important in gelating systems. Two simplifying assumptions of the FS theory are the following:

- (i) the absence of solvent molecules, and
- (ii) the absence of correlations between the molecules.

Both solvent effects and correlations are taken into account in this paper.

A. Solvent effects

Suppose we allow the sites to be of two sorts, A and B . A sites are occupied by monomers and B sites by solvent. The original "random-bond" percolation problem is now a "random-site-bond" problem¹⁸; the FS critical point in the simple phase diagram of Fig. 4(b) is now an entire "line" of critical points (Fig. 6). If p_s is the density of A sites, then FS theory corresponds to the special case $p_s = 1$ (heavy solid line). A typical experiment cor-

responds to moving to the right along the horizontal dashed line.

B. Correlations among molecules

We shall assume that the monomers and solvent molecules are *not* randomly distributed among the sites. Rather, we shall assume a correlation of the standard lattice-gas model sort (Fig. 7). In specifying the interactions, we must consider that the monomers can interact with each other in two ways. One is the usual van der Waals interaction, and the other is a directional interaction that leads to chemical bonds.

The particle-particle interaction of this system is reasonably approximated by the following nearest-neighbor interactions: $-W_{AA}$, the solvent-solvent interaction energy, $-W_{AB}$, the monomer-solvent interaction energy, and

$$-\epsilon_{BB} = \begin{cases} -W_{BB} \\ -E. \end{cases} \quad (1)$$

where $-W_{BB}$ is the van der Waals energy (weight p_u) and $-E$ is the bonding energy (weight $1-p_u$).

The interaction $-\epsilon_{BB}$ needs some further justification. Two monomers can interact in two different ways. The first is the usual van der Waals type of attraction, which we have approximated with a nearest-neighbor attraction $-W_{BB}$. The

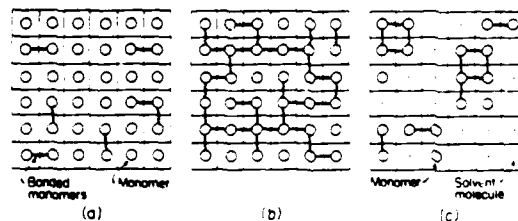


FIG. 7. (a) and (b) All sites are occupied by monomers (open circle), as in the Flory-Stockmayer model of gelation. The wavy lines correspond to chemical bonds between two monomers, while p_b is the probability of such a bond being present. (c) The model of gelation proposed here. Each site can be occupied by either a monomer (circle) or a solvent molecule (dot). The wavy line corresponds to a reversible bond. We find p_b , given by Eq. (12), is a function of the temperature. The monomers are correlated.

second is the interaction which leads to bonds (e.g., hydrogen bonds), which we have approximated with another nearest-neighbor interaction $-E$ or $-W_{BB}$. Of course this second interaction occurs only when the monomers are in a particular configuration. For a given pair of nearest-neighbor monomers, the ratio between the number of configurations N_E which lead to hydrogen bonding (energy $-E$) and the number of configurations N_{BB} which do not; $N_E/N_{BB} = (1-\rho_u)/\rho_u$ should therefore be much less than unity. Note that the entropy difference between the unbound state (with energy $-W_{BB}$) and unbound state (with energy $-E$) is given by

$$S = k_B \ln \rho_u / (1 - \rho_u).$$

The Hamiltonian for a system of N_A molecules of solvent and N_B monomers can be written as

$$- \mathcal{H}(N_A, N_B) = \sum_{\langle ij \rangle} [W_{AA} \Pi_i^A \Pi_j^A + \epsilon_{BB} \Pi_i^B \Pi_j^B + W_{AB} (\Pi_i^A \Pi_j^B + \Pi_i^B \Pi_j^A)] \quad (2)$$

The sum is over all possible AA , BB and AB nearest-neighbor pairs, where $\Pi_j^A = 1$ if site j is occupied by a solvent molecule, and $\Pi_j^A = 0$ otherwise. Similarly $\Pi_j^B = 1$ if site j is occupied by a monomer; $\Pi_j^B = 0$ otherwise. Since each cell must be occupied by either a solvent or a monomer, we have the constraint

$$\Pi_j^A + \Pi_j^B = 1. \quad (3)$$

The partition function $Z_N \{ \epsilon_{BB} \}$ for a given configuration of interacting bonds $\{ \epsilon_{BB} \}$ can be written

$$Z_N \{ \epsilon_{BB} \} = \sum_{N_A} \sum_{\text{conf}} \exp \{ \beta [\mu_A N_A + \mu_B N_B - \mathcal{H}(N_A, N_B)] \}, \quad (4)$$

where $\beta = 1/k_B T$, while μ_A and μ_B are the chemical potentials of species A and B . The first sum is over all the monomer-solvent configurations with N_A and N_B fixed. The second sum is over all values of $N_A = N - N_B$. By averaging over all possible energies of interaction ϵ_{BB} one obtains the partition function Z_N for this model of reversible gelation

$$Z_N = \overline{Z_N(\epsilon_{BB})}. \quad (5)$$

The partition function (5) can also be regarded as an annealed random-bond ferromagnetic problem.

Using the identities

$$N_A = \sum_j \Pi_j^A, \quad N_B = \sum_j \Pi_j^B, \quad (6)$$

and Eq. (3), we can write Eq. (4) in the form

$$Z_N \{ \epsilon_{BB} \} = Z_s \sum_{\{ \Pi_j^B \}} \exp \left\{ \beta \left[\mu_{\text{eff}} \sum_j \Pi_j^B + \alpha(\epsilon_{BB}) \sum_{\langle ij \rangle} \Pi_i^B \Pi_j^B \right] \right\}. \quad (7)$$

Here

$$Z_s = \exp \{ \beta [(f/2) N W_{AA} + \mu_A N] \} \quad (8a)$$

is the partition function of the pure solvent,

$$\mu_{\text{eff}} = \mu_B - \mu_A + f(W_{AB} - W_{AA}) \quad (8b)$$

and

$$\alpha(\epsilon_{BB}) = \epsilon_{BB} + W_{AA} - 2W_{AB}. \quad (8c)$$

The sum in (7) is over all possible configurations of monomers $\{ \Pi_j^B \}$. Equation (5) can be written

$$Z_N = Z_s \sum_{\{ \Pi_j^B \}} \exp \left\{ \beta \left[\mu_{\text{eff}} \sum_j \Pi_j^B + W \sum_{\langle ij \rangle} \Pi_i^B \Pi_j^B \right] \right\}, \quad (9)$$

where

$$\begin{aligned} e^{\beta W} &= \rho_u \exp[\beta \alpha(W_{BB})] + (1 - \rho_u) \exp[\beta \alpha(E)] \\ &= \rho_u \exp[\beta(W_{AA} + W_{BB} - 2W_{AB})] + (1 - \rho_u) \exp[\beta(E + W_{AA} - 2W_{AB})]. \end{aligned} \quad (10)$$

Equation (9) is obtained using the identity

$$\rho_u e^{\beta \alpha(W_{BB}) \Pi_i^B \Pi_j^B} + (1 - \rho_u) e^{\beta \alpha(E) \Pi_i^B \Pi_j^B} = e^{\beta W \Pi_i^B \Pi_j^B}. \quad (11)$$

In conclusion, our system is equivalent to a one-component system with an effective chemical potential μ_{eff} given by (8b) and effective energy W given by (10). From the partition function one can derive the free energy and all the thermodynamic

properties of the system. In particular, one can locate the consolute temperature T_c below which the system separates in the different phases, and the coexistence curve.

One interesting question is "can we derive the gelation curve from the free energy?" That is, in a temperature-density plane, can we derive from the free energy the curve which separates the sol phase from the gel phase? The answer is no for the model that we are considering. In fact the process of gelation is related to the connectivity properties of the system; connectivity properties have never been derived from a free energy.

A "gel" phase is defined to be the phase where a nonzero fraction of monomers are bonded together via chemical bonds to form a macroscopic molecule. In order to calculate the gelation threshold $\phi_g(T)$ we must specify when a pair of monomers are bonded. We require that (i) they be nearest neighbors and (ii) their relative energy be $-E$. Where two nearest-neighbor monomers satisfy (ii), we say that a bond is present between two monomers. The probability p_B that such a bond is present between two nearest-neighbor monomers can be easily calculated and is simply given by¹⁹

$$p_B = \frac{[(1-\rho_u)e^{BE}]}{[\rho_u e^{Bw_{BB}} + (1-\rho_u)e^{BE}]} \quad (12)$$

The reversible gelation that we are describing is an equilibrium situation where bonds are continuously created and destroyed on a time scale short compared to most observations (weak gels). It definitely does not apply to strong gels. Thus the time scales of weak gels are analogous to those of annealed random magnets, while strong gels are analogous to quenched random magnets.²⁰

The problem of calculating $\phi_g(T)$ is in some respects analogous to the usual site- or bond-percolation problem.⁷ However, it is more complex for the following two reasons: (a) In the "pure" site-percolation problem, the particles are randomly distributed, while here they are correlated according to the Hamiltonian (2) ("correlated" percolation). (b) In site percolation, the vertices can be occupied or not and the bonds are always present. In bond percolation the vertices are all occupied by the particles and the bonds may be present or absent. In our model the vertices may be occupied or not and also the bonds may be present or absent ("site-bond" percolation). The correlated percolation problem²¹⁻²⁵ and the site-bond percolation problem¹⁸ have each been treated separately, while we have proposed treating both

problems simultaneously.⁸

From the above considerations, it follows that if $p_B < p_c$, where p_c is the pure bond-percolation threshold, there is no gelation no matter how high the monomer density. Therefore from Eq. (12) there exists a limiting value of the temperature T_{max} , with $p_B(T_{max}) = p_c$ above which there is no gelation. From Eq. (12) it follows that T_{max} does not depend on the nature of the solvent.

Thus far we have presented a model to describe the sol-gel phase transition for weak gels. An explicit expression for p_B as function of temperature has been obtained and a value of temperature T_{max} , independent of solvent, is predicted above which there is no gel. In the next two sections we will solve this model for the interior of the Cayley tree. We will first calculate the equation of state (Sec. III) and then the connectivity properties (Sec. IV). Results on this lattice correspond to making Flory's assumption of no intramolecular interactions and hence the closed-form expressions we obtain provide a useful anchor point for theoretical descriptions of this model system.

III. EQUATION OF STATE ($M = 1$)

In the preceding section we have shown that the monomer-solvent solution is equivalent to an effective one-component system with the partition func-

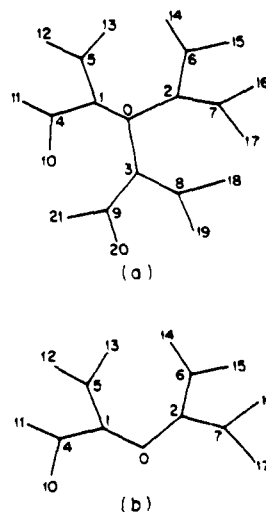


FIG. 8. (a) Cayley tree of coordination number $f = 3$. The center 0 is connected to branches with origin in 1, 2, 3. (b) Example of branch with origin in 0.

tion given by Eq. (9). For such a system we calculate here the equation of state for the interior of the Cayley tree, following closely the procedure of Ref. 24.

To fix the ideas, consider the Cayley tree or Bethe lattice of coordination number ("functionality") $f = 3$, with a "center" denoted 0 [Fig. 8(a)]. Any site is connected to f branches. Any bond, if cut, divides the tree in two branches. For example, if we cut the bond [03] we have one branch with origin 0 [Fig. 8(b)] and another with origin at 3.

We split the partition function $Z_N = Z_N(+)$ $- Z_N(-)$ where $Z_N(+)$ [$Z_N(-)$] is the partition function under the condition that site 0 is occupied (empty). They satisfy the following relations:

$$Z_N(+) = Z_{N_0}(+) [e^{\beta W} Z_{N_3}(+) + Z_{N_3}(-)], \quad (13a)$$

$$Z_N(-) = Z_{N_0}(-) [Z_{N_3}(+) + Z_{N_3}(-)], \quad (13b)$$

where $Z_{N_0}(+)$ [$Z_{N_0}(-)$] is the partition function of the branch 0 [Fig. 8(b)] under the condition that site 0 is occupied (empty). Analogous definitions hold for the partition function relative to branch 3. N_0 and N_3 are the number of sites, respectively, in branch 0 and 3. The density of monomers ϕ is clearly

$$\phi = \lim_{N \rightarrow \infty} [Z_N(+)] / [Z_N(+) + Z_N(-)]. \quad (14)$$

From Eqs. (13) and (14)

$$\phi = [y(ye^{\beta W} + 1)] / [y^2 e^{\beta W} + 2y + 1], \quad (15)$$

where

$$y = \lim_{N_0 \rightarrow \infty} [Z_{N_0}(+) / Z_{N_0}(-)] \\ = \lim_{N_3 \rightarrow \infty} [Z_{N_3}(+) / Z_{N_3}(-)]. \quad (16)$$

Here we have made the assumption of translational invariance. The translational invariance condition is equivalent to neglecting the surface of the Cayley tree.

We need an equation for y . To do so we write the following relations:

$$Z_{N_0}(+) = e^{\beta \mu_A} \prod_{i=1}^2 [e^{\beta W} Z_{N_i}(+) + Z_{N_i}(-)], \quad (17a)$$

$$Z_{N_0}(-) = \prod_{i=1}^2 [Z_{N_i}(+) + Z_{N_i}(-)]. \quad (17b)$$

Here we have introduced the partition functions

for the branches 1 and 2 which have been obtained by cutting, respectively, bonds [01] and [02].

Dividing Eq. (17a) by Eq. (17b) and using the translational invariance assumption, we obtain in the thermodynamic limit the desired expression for y .

$$y = e^{\beta \mu_A} (ye^{\beta W} + 1)^2 / (y + 1)^2. \quad (18)$$

A. General functionality

First we introduce the new variables

$$z = e^{-\beta W / 2}, \quad (19a)$$

$$\mu = e^{\beta \mu_A} z^{-f}, \quad (19b)$$

$$\mu_1 = y / z. \quad (19c)$$

Equations (15) and (18), generalized to arbitrary functionality f , become

$$\phi = (\mu_1^2 + \mu_1 z) / (\mu_1^2 + 2\mu_1 z + 1), \quad (20a)$$

$$\mu = \mu_1 [(\mu_1 z + 1) / (\mu_1 + z)]^{f-1}, \quad (20b)$$

which are the desired equations of state coinciding with the Bethe approximation.²⁴ From (19a), (19b), and (8b), μ can be written in the following way:

$$\mu = \exp \{ \beta [\mu_B + \mu_B(0)] - [\mu_A + \mu_A(0)] \}, \quad (21a)$$

where $\mu_B(0) = (\frac{1}{2})f\bar{W}_{BB}$ and $\mu_A(0) = (\frac{1}{2})f\bar{W}_{AA}$ are the chemical potential of species B and A , respectively, in the absence of species A and B .²⁶ Here

$$e^{\beta \bar{W}_{BB}} = \rho_B e^{\beta W_{BB}} + (1 - \rho_B) e^{\beta E}. \quad (21b)$$

From (20a) it follows that $\mu = 1$ corresponds to the disordered phase. The consolute temperature T_c (or equivalently z_c) and the consolute density ϕ_c are obtained from the equations:

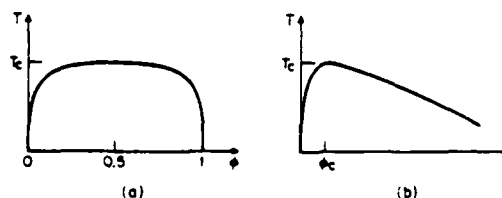


FIG. 9. (a) Coexistence curve for the monomer case ($M = 1$) and (b) for the polymer case ($M > 1$).

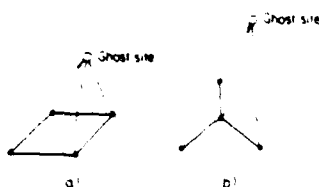


FIG. 10. Example of ghost sites for a section of the square lattice (a) and Cayley tree (b).

$$\frac{\partial \mu}{\partial \phi} = 0 \quad \text{or} \quad \frac{\partial \mu}{\partial \mu_1} = 0 \quad (22a)$$

and

$$\frac{\partial^2 \mu}{\partial \phi^2} = 0 \quad \text{or} \quad \frac{\partial^2 \mu}{\partial \mu_1^2} = 0 \quad (22b)$$

From Eqs. (20a), (20b), (22a), and (22b) we have

$$z_c = (f - 2)/f, \quad \phi_c = \frac{1}{2} \quad (23)$$

The spinodal curve ϕ_s is obtained from Eqs. (20a) and (22a),

$$\phi_s = (\mu_{1s}^2 + \mu_{1s}z) / (\mu_{1s}^2 + 2\mu_{1s}z + 1) \quad (24)$$

Here μ_{1s} is the solution of Eq. (22a) and is given by

$$\mu_{1s} = \frac{1}{2} F \pm (\frac{1}{4} F^2 - 1)^{1/2} \quad (25a)$$

and

$$F = z^{-1}(f - 2 - fz^2) \quad (25b)$$

The + and - signs in (25a) correspond to the two different branches of the spinodal curve. The coexistence curve is obtained by putting $\mu = 1$ and solving (20a) and (20b) for ϕ_{coex} as function of T (Fig. 9).

IV. CONNECTIVITY PROPERTIES

In this section we investigate the connectivity properties of the system. In particular, we are interested in the following quantities: (i) the percolation probability P , defined to be the probability that a given monomer belongs to the infinite cluster, (ii) the mean cluster size S ,

$$S = \sum s^2 n_s / \sum s n_s \quad (26)$$

Here n_s is the average number of clusters (molecules) per site of s monomers.

To calculate P we follow closely the formalism introduced by Essam²⁷ for random percolation and

extended by Coniglio^{22,24} for correlated percolation. Here we calculate P in the presence of the "ghost" field h (Refs. 28 and 29) which plays the same role as the magnetic field in a ferromagnet. To be more precise,²⁹ we introduce a ghost site which is connected to every site with probability h (see Fig. 10). Consequently all the sites that are connected with the ghost sites are connected to an infinite cluster. The advantage of introducing the ghost field stems from the relation²⁸

$$S = (1 - P)^{-1} \left[\frac{\partial P}{\partial h} \right]_{h=0} \quad (27)$$

Starting from the origin of the elementary cell [Fig. 8(a)] there are f branches that emanate from the origin. Given that the origin is occupied by a monomer, let Q be the probability that moving along one of the branches there is no infinite cluster attached to the origin. The probability P that the origin, occupied by a monomer, belongs to an infinite cluster is given by

$$P = 1 - (1 - h)Q^f \quad (28)$$

Clearly Q satisfies the following relation

$$Q = 1 - ap_B + ap_B(1 - h)Q^{f-1} \quad (29)$$

where a is the probability that one of the peripheral sites of the elementary cell [e.g., site 1 of Fig. 8(a)] is occupied under the condition that the origin is occupied,

$$a = \langle \Pi_0^B \Pi_1^B \rangle / \langle \Pi_0^B \rangle \quad (30)$$

where the angle brackets stand for the usual statistical average

$$\langle \dots \rangle = \sum_{\text{conf}} \dots e^{-\beta x} / \sum_{\text{conf}} e^{-\beta x} \quad (31)$$

Now a has already been calculated,²⁴ with the result

$$a = \mu_1 / (\mu_1 + z) \quad (32)$$

where z is given by Eq. (19a) and μ_1 by Eqs. (19c) and (20b) (see also Appendix A for a more general case $M \neq 1$). p_B is the probability that the two monomers at the origin 0 and at the peripheral site 1 are in a "bound state," and is given by Eq. (12). From (27)–(29), we have

$$S = \frac{(1 + ap_B Q^{f-2})}{[1 - (f-1)ap_B Q^{f-2}]} \quad (33)$$

where Q is calculated for $h = 0$.

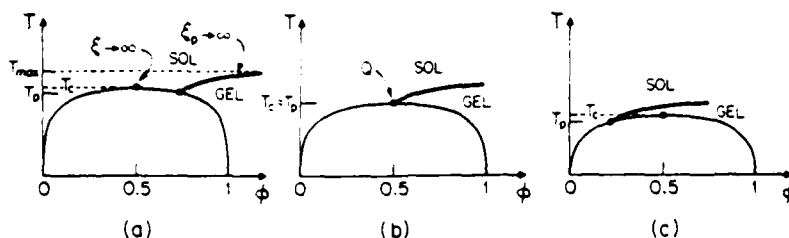


FIG. 11. Coexistence curve for the monomer-solvent binary mixture and sol-gel phase boundary for three different solvents ($M = 1$). The solvents have been chosen in such a way that the consolute point is (a) in the sol phase (b) on the gelation curve, and (c) in the gel phase. T_p is the temperature at which the gelation curve meets the coexistence curve. The situation depicted in (c) is not expected to be observable for usual experimental time scales.

We note that (29) is the same equation as for random site percolation. In this case ap_B becomes the monomer density ϕ . The equation for $h = 0$ has been studied previously.²⁷

The solution near the percolation threshold is

$$Q(x) = 1, \quad x < x_c \quad (34a)$$

$$Q(x) \sim 1 - [2/(f-2)]\epsilon, \quad x > x_c. \quad (34b)$$

Here $x_c = (f-1)^{-1}$, $x = ap_B$, and $\epsilon = (x - x_c)/x_c$. From Eqs. (28), (29), and (33), it follows that for $x > x_c$,

$$P \cong [2f/(f-2)]\epsilon \quad (35a)$$

and

$$S \cong f/|\epsilon|. \quad (35b)$$

The equation for the gelation threshold ϕ_g is determined by the condition

$$ap_B = (f-1)^{-1}. \quad (36)$$

From Eqs. (20a) and (32) we find

$$\phi_g = z^2 p_B (f-1) / \{ [p_B (f-1) - 1]^2 + z^2 [2(f-1)p_B - 1] \}, \quad (37)$$

which is identical to the critical threshold in the pure correlated case. The only difference is the change of $(f-1) \rightarrow (f-1)p_B$. We see that the bond dilution reduces the effective connectivity of the lattice. We also note that, consistent with our general result, we find, from (36) and from the fact that $z < 1$, the limiting value of the temperature T_{max} above which there is no gelation:

$$p_B(T_{max}) = (f-1)^{-1}. \quad (38)$$

Note that $(f-1)^{-1}$ is the percolation threshold for the pure random bond percolation.

In Fig. 11 we have plotted the sol-gel phase

boundary, Eq. (37), together with the coexistence curve for the binary mixture of monomers and solvent, for three good solvents. Changing the solvent corresponds to changing the parameters $W_{BB} - 2W_{AB}$. The solvent parameters have been chosen in such a way that the consolute point is in the sol region [Fig. 11(a)], on the gelation curve [Fig. 11(b)], and in the gel region [Fig. 11(c)]. We stress two interesting features:

(i) For all solvents there is a temperature T_p (below the consolute temperature T_c) at which the coexistence curve crosses the gelation curve. For $T < T_p$ we have coexistence between sol phase and gel phase. In addition, in Fig. 11(c) for $T_p < T < T_c$ we have two possible gel phases. Note that in a real system, this situation is very difficult to realize because the monomers form very large clusters for short time scales when the demixion concentration ϕ_c is near the gel curve. Therefore ϕ_c tends to decrease. Hence the situation depicted in Fig. 11(c) is not expected to be realized in practice.³⁰ Only for an infinite time scale, the monomers act as single elements and phase separation would occur at ϕ_c .

(ii) By changing the solvent properties it is possible to realize the interesting case in which the consolute point lies on gel-sol phase boundary, as shown in Fig. 11(b). We find that this special point Q is realized, if for fixed values of the solute parameters (ρ_u, E, W_{BB}) the solvent parameters ($W_{AA} - 2W_{AB}$) and T_c are related by

$$p_B = 1 - e^{-W/2kT_c} \equiv 1 - z_c. \quad (39a)$$

In fact, from (37) using (39a) and $z = z_c = f/(f-2)$ we find $\phi_g = \frac{1}{2}$. This means that critical point and gelation threshold coincide. Equation (39a) is actually valid for any lattice and for all d .³¹

This particular point Q is characterized by the

divergence of two lengths. One is the usual correlation length ξ which diverges at the consolute point, and the other is the characteristic linear dimension of the finite clusters (the "connectedness length") ξ_p which diverges on the sol-gel phase boundary. It is interesting to study the nature of point Q , which in some respects is analogous to the point $(T=0, p=p_c)$ in the $T-p$ phase diagram of a randomly dilute ferromagnet.

From Eqs. (35a) and (35b) we see that along all the gelation curve, including the Q point, the percolation critical exponents are the classical ones if the parameter $x = ap_B$ is chosen as variable. Experimentalists, however, do not measure exponents along a path of varying x but, for example, along the T axis. Therefore let us choose the value of p_B , given by Eq. (39a), so that we obtain the situation in which the Q point occurs. We can approach the Q point along the coexistence curve ($\mu=1$) using as variable $|T-T_c|$. We find critical exponents different from those that we find if we approach the Q point from $T > T_c$. In order to show this we must calculate near T_c

$$x - x_c = p_B a (\mu_{1,z}) - (f-1)^{-1}, \quad (39b)$$

with p_B given by Eq. (39a), $a(\mu_{1,z})$ given by Eq. (32), and μ_1 from Eq. (20b) with $\mu=1$. It is straightforward but tedious to show that $x - x_c \sim T - T_c$ for $T > T_c$ and $x - x_c \sim (T_c - T)^{1/2}$ for $T < T_c$ along the coexistence curve. Consequently the mean cluster size diverges with a classical exponent $\gamma_p = 1$ for $T > T_c$ and with a different exponent $\gamma_p = \frac{1}{2}$ for $T < T_c$.

This asymmetry above and below T_c is not found in low dimensionality using a Migdal-Kadanoff renormalization-group approach.³¹ However the critical exponents are found to be given by random percolation exponents along the gelation curve, with a crossover to different behavior as the Q point is approached. This same kind of crossover has also been found near six dimensions using the ϵ -expansion technique,³² where the calculations have been done only in the disordered phase ($T > T_c$; $\mu=1$). More study therefore is required to fully understand the critical behavior near the Q point especially as a function of the dimensionality of the system.

V. POLYMERS IN A SOLVENT ($M > 1$)

In this section we want to extend the previous treatment to the case of a solution of polymers in a solvent. Treatment of chain percolation can also

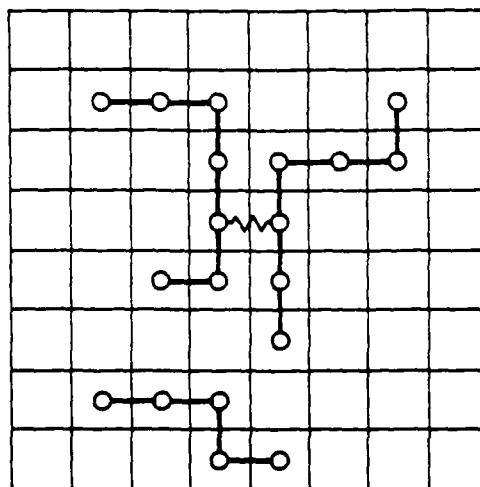


FIG. 12. Polymer chains embedded on a square lattice. The wavy line is a bond between two monomers of two different chains.

be found in Refs. 5 and 33. The polymer is made of M monomers, each one of which occupies a lattice site (Fig. 12). The solvent molecules, as in the case $M=1$, fill the remaining sites of the lattice. The monomer-monomer, solvent-solvent, and monomer-solvent interactions are given by Eq. (1) as before. The partition function becomes $Z_N\{\epsilon_{BB}\}$ for a given configuration of monomer interaction $\{\epsilon_{BB}\}$ can be written as:

$$Z_N\{\epsilon_{BB}\} = Z_s \sum_{n=0}^{\infty} Z_n\{\epsilon_{BB}\}. \quad (40a)$$

Here Z_s is the partition function of the pure solvent, given by Eq. (8a), while Z_n is the contribution to the partition function which comes from those configurations with n polymers,

$$Z_n\{\epsilon_{BB}\} = e^{\beta\mu_{eff}n} \sum_{\text{config}} e^{\beta\sum \epsilon_{BB} N_{BB}}. \quad (40b)$$

The sum is over all configurations of the n polymers, N_{BB} is the number of nearest-neighbor pairs of monomers, and

$$\begin{aligned} \mu_{eff} &= \mu_{poly} - M\mu_A \\ &- [(f-2)M+2](W_{AA}-W_{AB}) \\ &- (M-1)W_{AA}. \end{aligned} \quad (41)$$

where μ_{poly} and μ_A are the chemical potentials, respectively, of the polymer and the solvent. The origin of (41) can be easily understood considering

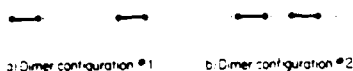


FIG. 13. Examples of configurations of two dimers (a) without nearest-neighbor monomers and (b) with two nearest-neighbor monomers.

the example of two dimers ($n = 2, M = 2$), as illustrated in Fig. 13. There are two possible configurations. We have to calculate the energy and the chemical potential of a system made of $(N - 4)$ solvent molecules. Since the contribution to the chemical potential is $\mu_A N$ in Z_s , we must subtract such a term and add $n\mu_{\text{poly}}$ due to the presence of two polymer molecules. The contribution to (41) due to the chemical potential is

$$n\mu_{\text{eff}}^{(1)} = n\mu_{\text{poly}} - nM\mu_A. \quad (42)$$

The contribution to (41) due to the interaction is

$$W^{(1)} = n[(f-2)M+2](W_{AA} - W_{BB}) + (M-1)W_{AA} + N_{BB}(W_{AA} - 2W_{AB} + \epsilon_{BB}). \quad (43)$$

The sum $n\mu_{\text{eff}}^{(1)} + W^{(1)} = n\mu_{\text{eff}} + (\epsilon_{BB})N_{BB}$ proves Eqs. (40) and (41).

Taking in (40b) the average over all possible values of ϵ_{BB} , the partition function $Z_N = Z_N\{\epsilon_{BB}\}$ becomes

$$Z_N = Z_s \sum_n Z_n. \quad (44a)$$

Here

$$Z_n = e^{\beta n \mu_{\text{eff}}} \sum_{\text{conf}} e^{\beta n W_{BB}}, \quad (44b)$$

where W is given by Eq. (8c).

In conclusion, the partition function of our sys-

tem is equivalent to the grand partition function of a system of polymers with an effective chemical potential μ_{eff} given by Eq. (41) and an effective monomer-monomer interaction W given by Eq. (10).

As for the case $M = 1$, we derive the equation of state in closed form for the interior of the Cayley tree. The equation of state is derived in Appendix A. Here we give only the result for the monomer density ϕ ,

$$\phi = R(\mu_1^2 + \mu_1 z) / [R\mu_1^2 + (1+R)\mu_1 z + 1]. \quad (45)$$

Here

$$\mu = \mu_1(\mu_1 z + 1)^{M(f-1)} / (\mu_1 + z)^{M(f-2)+1}, \quad (46a)$$

$$R = \frac{f(f-1)}{[(f-1)(f-2) + 2(f-1)/M]}, \quad (46b)$$

and

$$\mu = \exp\{\beta[\mu_{\text{poly}} + \mu_{\text{poly}}(0)] - M[\mu_A + \mu_A(0)]\}, \quad (46c)$$

where $\mu_{\text{poly}}(0)$ is the chemical potential of the polymers in absence of solvent, and $\mu_A(0)$ is the chemical potential of the solvent in absence of polymers; explicit expressions are in Appendix A and z has been defined in Eqs. (19a) and (10). If we set $M = 1$, Eqs. (45) and (46) reduce to Eqs. (20a) and (20b) derived in Sec. III.

The consolute temperature T_c , or equivalently z_c , is obtained from the two equations

$$\frac{\partial \mu}{\partial \phi} = 0 \quad (\text{or equivalently, } \frac{\partial \mu}{\partial \mu_1} = 0), \quad (47a)$$

$$\frac{\partial^2 \mu}{\partial \phi^2} = 0 \quad (\text{or equivalently, } \frac{\partial^2 \mu}{\partial \mu_1^2} = 0). \quad (47b)$$

From Eqs. (45) and (47) we find

$$z_c = -M^{1/2} / [M(f-1)+1] + [M(f-1)+1]^{-1} [M^2(f-1)^2 - M^2(f-1) + M(f-1) + M-1]^{1/2} \quad (48a)$$

and

$$\phi_c = (R + RM^{1/2}z_c) / [R + (1+R)M^{1/2}z_c + M]. \quad (48b)$$

Clearly for large M ,

$$z_c \sim (f-1)^{-1} [(f-1)(f-2)]^{1/2}$$

and $\phi_c \sim Rz_c M^{-1/2}$.

The spinodal curve ϕ_s can be obtained from Eqs. (45) and (47a)

$$\phi_s = R(\mu_{1s}^2 + \mu_{1s}z) / [R\mu_{1s}^2 + (1+R)\mu_{1s}z + 1], \quad (49)$$

where μ_{1s} is the solution of Eq. (47a) and is given by

$$\mu_{1s} = F/2 \pm (F^2/4 - M^{-1})^{1/2} \quad (50a)$$

and

$$F = -\{M(f-1)+1\}z^2 - M(f-2)/Mz \quad (50b)$$

For the case $M=1$, in order to find the coexistence curve ϕ_{coex} , it was enough to put $\mu=1$ because of the symmetry. This time we have to apply the "equal area" rule. The conditions for the coexistence curve are that the pressure P and the chemical potential must be the same in coexisting phases A and B . From the relation $dP/d\mu_{\text{eff}} = \rho$, where ρ is the density of chains related to the density of monomers by $\phi = M\rho$. The condition for the pressure to be the same is

$$\int_A^B dP = \int_A^B \rho d\mu_{\text{eff}} = 0$$

or

$$\int_A^B \phi d(\ln \mu) = 0,$$

and for the chemical potential $\mu(A) = \mu(B)$. In Fig. 14 we have plotted schematically ϕ_{coex} as a function of T . Note that the critical density ϕ_c is located much nearer to zero than in the symmetric case $M=1$ (Fig. 9).

The connectivity properties of the system of chains can also be derived. Here we give only the result for the gelation curve ϕ_g (the derivation is given in Appendix B),

$$\phi_g = Rz^2(\bar{f}-1)/\{[(1+R)(\bar{f}-1) - 1]z^2 + (\bar{f}-2)^2\}. \quad (51)$$

Here

$$\bar{f}-1 = [M(f-1)+1-M]p_B, \quad (52)$$

and p_B is given by Eq. (20b). The discussion of the results for $M > 1$ is identical to the $M=1$ case, and the results are indicated in Fig. 14.

VI. SUMMARY

In conclusion we have proposed a model which applies to weak gels. We have solved the model in closed form for the Cayley tree. The general phase diagrams are in qualitative agreement with the experimental data of Tanaka *et al.*³⁴ and Ruiz *et al.*³⁵ This model can also be adapted to explain peculiar effects inherent in the $M \gg 1$ system.³⁶ An interesting situation occurs when for a particular solvent the gelation curve ends at the consolute point. This point is a higher-order critical point where both the correlation length and the connectiveness length diverge.

In the Cayley-tree solution, which is valid for high dimensionality, the critical behavior in the sol-gel transition exhibits an asymmetry above and below the consolute temperature. This asymmetry is not found in a renormalization-group approach in low dimensionality.³¹ More study needs to be done to investigate the nature of this Q point as function of the dimensionality. This point presents analogies with the end of the line of critical points in the dilute ferromagnets. Such lines of critical points cannot be obtained with the previous simplified theory of gelation.

After this work was completed, several extensions of the present model were developed. In particular, Barrett³⁷ has recently generalized the present model to incorporate features displayed by the polymeric system hyaluronic acid, which undergoes an order-disorder transition. There are two types of side groups, amide and carboxyl, as well as two types of "solvent molecules," potassium ions and phosphate ions. Very recently, Delyon *et al.*³⁸ found that the present model displays a peculiar transition in the region below T_c . A physical interpretation of this effect has been suggested by Klein and Stauffer.³⁹

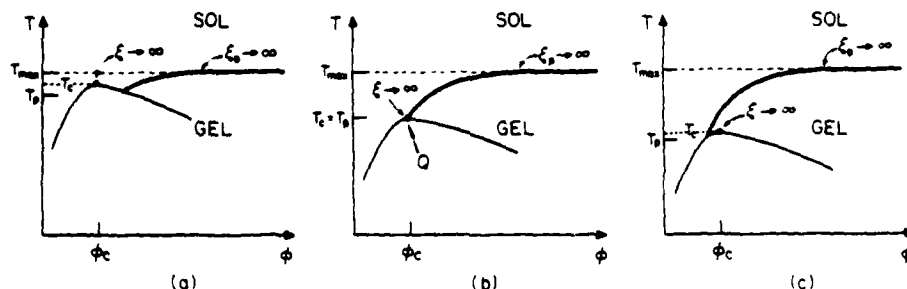


FIG. 14. Same as Fig. 11 except that M is large (polymer).

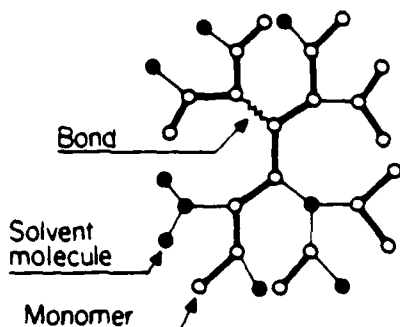


FIG. 15. Polymer chains (heavy line) embedded on a Bethe lattice of coordination number $f=3$. The open circles are the monomers. The dots are the solvent molecules. The wavy lines are the bonds between monomers of different chains.

The special case of the present model in which bonds are considered broken with probability

$$q_B = 1 - p_B = \exp(-2J/kT)$$

was introduced by Coniglio and Klein³¹ as a candidate for representing "droplets" at the critical point of an Ising model with coupling constant J . Numerical studies in two and three dimensions indicate that these site-bond percolation clusters in fact do behave just like Ising droplets in that their spatial extent becomes infinite at the critical point.⁴⁰ Thus we see that a model introduced in connection with polymer gelation would appear to be of relevance for a completely different problem—that of defining Ising droplets near the critical point of a thermal phase transition.

ACKNOWLEDGMENTS

This work was stimulated in large part by discussions with T. Tanaka, and we are particularly grateful for his communication of some of his extensive experimental results prior to their publication. We also acknowledge many extremely helpful conversations with P. Ruiz, D. Stauffer, S. Redner, F. Rys, R. Bansil, and P. J. Reynolds kindly commented on the manuscript. One of us (H.E.S.) is grateful to the John Simon Guggenheim Memorial Foundation for financial support during the time this work was being carried out. This work was supported in part by grants from Consiglio Nazionale delle Ricerche, NSF, Army Research Office, AFOSR, and ONR.

APPENDIX A: POLYMERS IN A SOLVENT, EQUATION OF STATE

Here we derive the equation of state of a solution of polymers in a solvent for the interior of the Cayley tree. The result was given in Sec. V, Eqs. (45) and (46). The polymer is made of M monomers, each one of which occupies a lattice site (Fig. 15). The partition function Z_n is given by Eqs. (44a) and (44b) which we recall here for convenience

$$Z_N = Z_0 \sum_{n=0} Z_n, \quad (\text{A1})$$

with

$$Z_n = e^{\beta \mu_{eff} n} \sum_{\text{config}} e^{\beta W N_{BB}}, \quad (\text{A2})$$

All the other quantities are defined in Sec. V.

Consider first the case $M=2$. Following the derivation for the $M=1$, we consider the Cayley tree of coordination number 3 [Fig. 8(a)] and write

$$Z_N = Z_N(-) + Z_N(+), \quad (\text{A3})$$

where $Z_N(-)$ and $Z_N(+)$ are the partition functions under the condition that the origin 0 is, respectively, empty or occupied by a monomer. In the latter case we can write

$$Z_N(+) = Z_N[0,1] + Z_N[0,2] + Z_N[0,3], \quad (\text{A4})$$

where $Z_N[0,i]$ ($i=1,2,3$) is the partition function under the condition that the dimer occupies bond $[0,i]$. The following relations hold:

$$Z_N[0,1] = e^{\beta \mu_{eff}} \prod_{i=2}^3 [e^{\beta W} Z_{N_i}(+) Z_{N_i}(-)], \quad (\text{A5})$$

$$Z_N(-) = \prod_{i=1}^3 [Z_{N_i}(+) + Z_{N_i}(-)]. \quad (\text{A6})$$

Here $Z_{N_i}(-)$ and $Z_{N_i}(+) = Z_{N_i}[2,6] + Z_{N_i}[2,7]$ are the partition functions of branch 2 under the condition that site 2 is, respectively, vacant or occupied by a monomer. $Z_{N_i}[2,6]$ and $Z_{N_i}[2,7]$ are the contributions relative to the configurations in which the dimer occupies, respectively, the bond $[2,6]$ and $[2,7]$. Analogous definitions hold for any other $Z_{N_i}(+)$ and $Z_{N_i}(-)$ and analogous relations hold for $Z_N[0,2]$ and $Z_N[0,3]$. We also have

$$Z_{N_i}(-) = [Z_{N_i}(+) + Z_{N_i}(-)][Z_{N_i}(+) + Z_{N_i}(-)]. \quad (\text{A7})$$

In relation to branch 0 [Fig. 8(b)] the following relations also hold:

$$\begin{aligned}
 Z_{N_0}[0,1] &= e^{\beta\mu_{N_0}}[e^{\beta W}Z_{N_1}(+) + Z_{N_1}(-)] \\
 &\quad \times [e^{\beta W}Z_{N_2}(+) + Z_{N_2}(-)] \\
 &\quad \times [e^{\beta W}Z_{N_3}(+) + Z_{N_3}(-)], \quad (\text{A8})
 \end{aligned}$$

$$Z_{N_0}(-) = [Z_{N_1}(+) + Z_{N_1}(-)]$$

$$\times [Z_{N_2}(+) + Z_{N_2}(-)]. \quad (\text{A9})$$

Taking the ratio (A8):(A9),

$$\frac{Z_{N_0}[0,1]}{Z_{N_0}(-)} = \frac{e^{\beta\mu_{N_0}}(e^{\beta W}y_{N_1}+1)(e^{\beta W}y_{N_2}+1)(e^{\beta W}y_{N_3}+1)Z_{N_1}(-)Z_{N_2}(-)}{(y_{N_1}+1)(y_{N_2}+1)Z_{N_1}(-)}, \quad (\text{A10})$$

where $y_{N_i} = [Z_{N_i}(-)]/[Z_{N_i}(+)]$ for any i . From (A7) and taking the limit $N_i \rightarrow \infty$, Eq. (A10) becomes

$$y/2 = e^{\beta\mu_{N_0}}(e^{\beta W}y+1)^3/(y+1)^4, \quad (\text{A11})$$

where

$$y = \lim_{N_i \rightarrow \infty} y_{N_i}.$$

Note that here we have assumed the independence upon the particular site i . This assumption is equivalent to neglecting the surface effects.

The monomer density ϕ in the thermodynamic limit is given by

$$\phi = \lim_{N \rightarrow \infty} Z_N(+)/Z_N. \quad (\text{A12})$$

From Eqs. (A3)–(A7)

$$\phi = 1 / \left[1 + 3e^{\beta\mu_{N_0}} \frac{(e^{\beta W}y+1)^4}{(y+1)^5} \right]. \quad (\text{A13})$$

From (A11)

$$\phi = \frac{\frac{1}{2}y(e^{\beta W}y+1)}{\frac{1}{2}y(e^{\beta W}y+1)+y+1}. \quad (\text{A14})$$

The above calculations can be easily generalized to chains made of M monomers on a Cayley tree of coordination number f . In this case Eqs. (A11) and (A14) become

$$y = \frac{ae^{\beta\mu_{N_0}}(e^{\beta W}y+1)^{M(f-2)+1}}{(y+1)^{M(f-1)}}, \quad (\text{A15})$$

$$\phi = \frac{(b/a)y(e^{\beta W}y+1)}{(b/a)y(e^{\beta W}y+1)+y+1}, \quad (\text{A16})$$

where

$$a = \frac{1}{2}(f-1)^{M-2}[(f-2)M+2]$$

is the number of ways of embedding a polymer

containing the origin on one branch of the Cayley tree [Fig. 8(b)] and

$$b = \frac{1}{2}(f-1)^{M-2}fM$$

is the number of ways of embedding a polymer containing the origin on the Cayley tree [Fig. 8(a)]. The above expressions for a and b , which are valid for $M \geq 2$, will be derived at the end of this appendix. If, for convenience, we introduce the following new variables,

$$z = e^{\beta W/2}, \quad (\text{A17})$$

$$\mu_1 = z^{-1}y, \quad (\text{A18})$$

$$\mu = a^{-1}e^{\beta\mu_{N_0} - M(f-2)-2}, \quad (\text{A19})$$

$$R = b/a$$

$$= \frac{f(f-1)}{[(f-1)(f-2)+2(f-1)/M]}, \quad (\text{A20})$$

Eqs. (A15) and (A16) become

$$\mu = [\mu_1(\mu_1 z + 1)^{M(f-1)}] / [(\mu_1 + z)^{M(f-2)} + 1], \quad (\text{A21})$$

$$\phi = [R(\mu_1^2 + \mu_1 z)] / [R\mu_1^2 + (1+R)\mu_1 z + 1]. \quad (\text{A22})$$

These two coupled equations represent the desired equation of state. Note that (A19) can be written in a different way. In fact, from (41), (A17), and (10),

$$\mu = e^{\beta[\mu_{\text{poly}} + \mu(0)] - M[\mu_A + \mu_A(0)]}, \quad (\text{A23})$$

where

$$\mu_{\text{poly}}(0) = -\ln a + \frac{1}{2}[M(f-2)+2]\bar{W}_{BB} \quad (\text{A24})$$

is the chemical potential of the polymers in absence of solvent, \bar{W}_{BB} is defined in Eq. (21b), and

$$\mu_A(0) = (f/2)W_{AA} \quad (\text{A25})$$

is the chemical potential of the solvent in absence of polymers.

Now we want to calculate explicitly the expression for $a \equiv a(M, f)$ and $b \equiv b(M, f)$. According to their definition we have

$$a(M, f) = \left[\frac{f-1}{2} \right] \sum_{M_1+M_2=M-1} g(M_1)g(M_2) + (f-1)g(M-1), \quad (\text{A26})$$

$$b(M, f) = \left[\frac{f}{2} \right] \sum_{M_1+M_2=M-1} g(M_1)g(M_2) + fg(M-1). \quad (\text{A27})$$

Here M_1 and $M_2 \geq 1$ and $g(K)$ is the number of configurations of embedding a chain of K bonds in a given branch with the origin fixed which is given by

$$g(K) = \begin{cases} (f-1)^{K-1}, & K \geq 1 \\ 1, & K = 0. \end{cases} \quad (\text{A28})$$

From (A26), (A27), and (A28) for $M \geq 2$,

$$a(M, f) = \frac{1}{2}(f-1)^{M-2}[(f-2)M+2],$$

$$b(M, f) = \frac{1}{2}(f-1)^{M-2}fM.$$

The ratio

$$R \equiv (b/a) = \frac{(f-1)f}{[(f-1)(f-2)+2(f-1)/M]}.$$

APPENDIX B: PERCOLATION OF INTERACTING CHAINS

Here we consider the connectivity properties of a system of chains made of M monomers. The monomers interact with an effective interaction given by Eq. (10). Two chains are bonded if they have at least two monomers bonded. The probability p_B for two nearest-neighbor monomers being bonded is given by Eq. (12).

We calculate now in the Cayley-tree approximation the gelation threshold $\phi_g(T)$, i.e., the minimum density of monomers above which a nonzero fraction of monomers are bonded together to form

a macroscopic molecule (infinite cluster). Consider first the case $M=2$, $p_B=1$. If P is the probability that the origin 0 [Fig. 8(a)] occupied by a monomer, belongs to an infinite cluster, then

$$P = \frac{P(01)+P(02)+P(03)}{[p(01)+p(02)+p(03)]}. \quad (\text{B1})$$

$P(0i)$ is the probability that there is a dimer in $(0i)$ and belongs to an infinite cluster ($i=1,2,3$); $\sum_i P(0i)$ is the fraction of monomers which belong to an infinite cluster, $p(0i)$ is the probability that there is dimer in $(0i)$ ($i=1,2,3$), $\phi = \sum_i p(0i)$ is the density of monomers. In the limit of infinite systems we have $P(01)=P(02)=P(03)$, and $p(01)=p(02)=p(03)$. Consequently $P=P(01)/p(01)$. This quantity can also be written as

$$P = 1 - Q_2 Q_3 Q_4 Q_5, \quad (\text{B2})$$

Q_2 is the probability that there is no infinite cluster in the branch (2.6)–(2.7) under the condition that site 0 is occupied by a monomer.

Also in the limit of infinite system we have $Q_2=Q_3=Q_4=Q_5 \equiv Q$. Let us calculate $Q_2=Q$,

$$Q = 1 - p_2(0 \text{ occup}) + p_2(0 \text{ occup})Q^3, \quad (\text{B3})$$

where $p_2(0 \text{ occup})$ is the probability that site 2 is occupied by a monomer under the condition that 0 is occupied by a monomer belonging to a different chain,

$$p_2(0 \text{ occup}) = \langle \Pi_{01} \Pi_2(+) \rangle / \langle \Pi_{01} \rangle$$

$$= \langle \Pi_{01} \Pi_2(+) \rangle / [\langle \Pi_{01} \Pi_2(+) \rangle + \langle \Pi_{01} \Pi_2(-) \rangle]. \quad (\text{B4})$$

where Π_{01} is the projector operator on states in which the polymer occupies position (01). $\Pi_2(+)$ and $\Pi_2(-)$ are the projector operators on states in which site 2 is, respectively, occupied or not by a monomer. The angle brackets stand for the thermal average. Using the same approach as in Appendix A we have

$$\langle \Pi_{01} \Pi_2(+) \rangle = (1/Z_N) Z_{N_0}[0,1] e^{\beta W} Z_{N_2}(+), \quad (\text{B5})$$

$$\langle \Pi_{01} \Pi_2(-) \rangle = (1/Z_N) Z_{N_0}[0,1] Z_{N_2}(-), \quad (\text{B6})$$

where $Z_{N_0}[0,1]$ is the partition function of the branch (0,1)–(0,3) [see Fig. 8(a)], under the condition that there is a dimer in (01). $Z_{N_2}(+)$ and $Z_{N_2}(-)$ are the partition functions of the other

branch with origin in 2 under the condition that site 2 is, respectively, occupied or empty.

From (B4) follows

$$p_2(0 \text{ occup}) = e^{\beta W} y / (e^{\beta W} y + 1) = \mu_1 / (\mu_1 + z). \quad (\text{B7})$$

Here y , μ_1 , and z have been defined in Appendix A. In the case of general M , Eq. (B2) becomes

$$P = 1 - Q^{\hat{f}}, \quad (\text{B8})$$

where $\hat{f} = M(\bar{f} - 2) + 2$. And Eq. (B3) becomes

$$Q = 1 - a + aQ^{\hat{f}-1} \quad (\text{B9})$$

and $a = \mu_1 / (\mu_1 + z)$. We introduce a probability p_B that there is a cross link between the nearest-neighbor monomers. Then Eq. (B9) becomes

$$Q = 1 - ap_B + ap_B Q^{\hat{f}-1}, \quad (\text{B10})$$

which is the same as Eq. (24) for $M = 1$ and $h = 0$ with an effective coordination number \bar{f} . The gelation threshold will therefore be given by

$$a_g = 1 / p_B(\hat{f} - 1), \quad (\text{B11})$$

namely

$$\mu_{1g} = z / [(\hat{f} - 1)p_B - 1], \quad (\text{B12})$$

which substituted in Eq. (A22) gives the gelation threshold

$$\phi_g = R z^2 (\bar{f} - 1) / \{ [(1 + R)(\bar{f} - 1) - 1] z^2 + (\bar{f} - 2)^2 \}, \quad (\text{B13})$$

where $\bar{f} - 1 = (\hat{f} - 1)p_B$.

*On leave from Gruppo Nazionale Struttura della Materia, Istituto di Fisica Teorica, Università di Napoli, Mastra D'Oltremare, Pad. 19, 80125 Napoli, Italy.

¹T. D. Lee and C. N. Yang, *Phys. Rev.* **87**, 410 (1952).

²R. Hocken and M. Moldover, *Phys. Rev. Lett.* **37**, 29 (1978); see also J. M. H. Levelt-Sengers, R. Hocken, and J. V. Sengers, *Phys. Today* **30** (12), 42 (1977).

³P. G. de Gennes, *Phys. Lett.* **38A**, 339 (1972).

⁴J. des Cloiseaux, *J. Phys. (Paris)* **36**, 281 (1975).

⁵For a review see, e.g., the recent authoritative monograph P. G. de Gennes, *Scaling Concepts in Polymer Physics* (Cornell University Press, Ithaca, 1979); a more concise review by the same author is *Riv. Nuovo Cimento* **7**, 363 (1972).

⁶M. E. Fisher and J. W. Essam, *J. Math. Phys.* **2**, 609 (1961); H. L. Frisch and J. M. Hammersley, *J. Soc. Ind. Appl. Math.* **11**, 894 (1963); P. G. de Gennes, *J. Phys. (Paris)* **36**, 1049 (1975); D. Stauffer, *J. Chem. Soc. Faraday Trans. 2*, 1354 (1976).

⁷See, e.g., the recent reviews D. Stauffer, *Phys. Rep.* **54**, 1 (1979); J. W. Essam, *Rep. Prog. Phys.* **43**, 833 (1980).

⁸A preliminary report of portions of the present work appeared in A. Coniglio, H. E. Stanley, and W. Klein, *Phys. Rev. Lett.* **42**, 518 (1979).

⁹See, e.g., the review article M. Gordon and S. B. Ross-Murphy, *Pure Appl. Chem.* **43**, 1 (1975).

¹⁰P. J. Flory, *J. Am. Chem. Soc.* **63**, 3083 (1941); **63**, 3091 (1941); **63**, 3096 (1941).

¹¹W. H. Stockmayer, *J. Chem. Phys.* **11**, 45 (1943).

¹²The classic sourcebook on polymer science is P. J. Flory, *Principles of Polymer Chemistry* (Cornell University Press, Ithaca, 1979).

¹³T. Vicsek and J. Kertész, *J. Phys. A* **14**, L31 (1981).

¹⁴E. T. Gawliniski and H. E. Stanley, *J. Phys. A* **14**, L169 (1981).

¹⁵U. Brauner, *Makromol. Chem.* **180**, 251 (1979).

¹⁶M. Schmidt and W. Burchard, *Macromolecules* **14**, 370 (1981).

¹⁷D. Stauffer, A. Coniglio, and M. Adam, *Adv. Poly. Sci.* (in press).

¹⁸P. Agrawal, S. Redner, P. J. Reynolds, and H. E. Stanley, *J. Phys. A* **12**, 2072 (1979); H. Nakanishi and P. J. Reynolds, *Phys. Lett.* **71A**, 252 (1979); J. Hoshen, P. Klymko, and R. Kopelman, *J. Stat. Phys.* **21**, 583 (1979).

¹⁹When $T \rightarrow \infty$, we expect on physical grounds that $p_B \rightarrow 0$, contrary to Eq. (12). In order to find the expected behavior, we can define the bond in a more sophisticated way, taking into account the kinetic energy [see, e.g., T. L. Hill, *Statistical Mechanics* (McGraw-Hill, New York, 1956), p. 156; and A. Coniglio, U. De Angelis, and T. Forlani, *J. Phys. A* **10**, 1123 (1977)]. This will lead to a new bond probability which differs from the previous one by an extra factor given by a ratio of gamma functions $\Gamma(\frac{1}{2}, E/kT) / \Gamma(\frac{1}{2})$ which approaches zero in the limit $T \rightarrow \infty$. However, this new bond probability essentially coincides with (12) in the range of temperature in which we are interested due to the fact that $(1 - \rho_u) / \rho_u < 1$.

²⁰C. Daoud and A. Coniglio, *J. Phys. A* **14**, L108 (1981).

²¹H. Müller-Krumbhaar, *Phys. Lett.* **50A**, 27 (1974).

²²A. Coniglio, *J. Phys. A* **8**, 1773 (1975).

²³W. Klein, H. E. Stanley, P. J. Reynolds, and A. Coniglio, *Phys. Rev. Lett.* **41**, 1145 (1979).

²⁴A. Coniglio, *Phys. Rev. B* **13**, 2194 (1976).

²⁵M. F. Sykes and D. S. Gaunt, *Phys. A* **9**, 2131 (1976); C. Domb and E. Stoll, *J. Phys. A* **10**, 1161 (1977).

²⁶See, e.g., Eq. (20.10) of T. L. Hill, *Introduction to*

- Statistical Thermodynamics* (Addison-Wesley, London, 1960), p. 373.
- ²⁷J. W. Essam, in *Phase Transitions and Critical Phenomena*, edited by C. Domb and M. S. Green (Academic, London, 1972), Vol. 2.
- ²⁸P. W. Kasteleyn, *J. Phys. Soc. Jpn.* **26**, 11 (1969); C. Fortuin and P. W. Kasteleyn, *Physica (Utrecht)* **57**, 536 (1972).
- ²⁹P. J. Reynolds, H. E. Stanley, and W. Klein, *J. Phys. A* **10**, L203 (1977).
- ³⁰J. F. Joanny, *Polymer* **21**, 71 (1980).
- ³¹A. Coniglio and W. Klein, *J. Phys. A* **13**, 2775 (1980).
- ³²A. Coniglio and T. C. Lubensky, *J. Phys. A* **13**, 1783 (1980).
- ³³T. C. Lubensky and J. Isaacson, *Phys. A* **20**, 2130 (1979); A. Coniglio and M. Daoud, *J. Phys. A* **12**, L259 (1979); M. Daoud, *J. Phys. Lett.* **40**, 201 (1979); G. Ord and S. Whittington, *J. Phys. A* **15**, L29 (1982).
- ³⁴T. Tanaka, G. Swislow, and I. Ohmine, *Phys. Rev. Lett.* **42**, 1557 (1979).
- ³⁵P. Ruiz, A. Coniglio, H. E. Stanley, W. Klein, and T. Tanaka, *J. Chem. Phys.* (unpublished).
- ³⁶A. E. Gonzalez and S. Muto, *J. Chem. Phys.* **73**, 4668 (1980).
- ³⁷A. E. Barrett, *Phys. Rev. Lett.* (in press).
- ³⁸F. Delyon, B. Souillard, and D. Stauffer, *J. Phys. A* **14**, L243 (1981).
- ³⁹W. Klein and D. Stauffer, *J. Phys. A* **14**, L413 (1981).
- ⁴⁰D. Stauffer, *J. Phys. Lett. (Paris)* **42**, L99 (1981); J. Roussenoq, *J. Aerosol Sci.* **12**, 432 (1982); H. Ottavi, *Z. Phys. B* **44**, 203 (1981); D. W. Heermann and D. Stauffer, *ibid.* **44**, 339 (1981).

ATE
LMED
— 8